# Evolution of the ferromagnetic and nonferromagnetic phases with temperature in phase-separated $La_{1-x}Sr_xCoO_3$ by high-field $^{139}La$ NMR

M. J. R. Hoch,[1] P. L. Kuhns, W. G. Moulton,[1] A. P. Reyes,[1] J. Lu,[1] J. Wu,[2] and C. Leighton[2]
[1]*National High Magnetic Field Laboratory, 1800 East Dirac Drive, Tallahassee, Florida 32310, USA*
[2]*Department of Chemical Engineering and Materials Science, University of Minnesota, Minneapolis, Minnesota 55455, USA*
(Received 16 June 2004; published 22 November 2004)

We have investigated microscopic magnetoelectronic phase separation and phase evolution with temperature in $La_{1-x}Sr_xCoO_3$, for $x$ in the range zero to 0.3, using high-field $^{139}La$ NMR. For $x \geqslant 0.1$ three coexisting magnetic phases, ferromagnetic (FM), paramagnetic (PM), and spin glass (SG) or cluster glass are observed in the spectra over a wide temperature range. The temperature evolution of the phases shows some conversion of SG to FM phase occurs as the temperature is raised above 30 K. This temperature range coincides with the interval in which Co ions undergo a low-spin (LS) to intermediate-spin (IS) state transition in undoped or very lightly doped material. Measurements on undoped and lightly doped ($x=0.03$) samples provide information on line shape, nuclear relaxation rates, and the LS to IS transition of the Co ions in the PM material. At high temperatures approaching the maximum measured Curie temperature of $\sim$240 K, found for $x \geqslant 0.3$, the FM phase signal changes and shifts significantly following the magnetization. Evidence for the existence of magnetic entities such as spin polarons coexisting with the PM phase is found at the higher temperatures.

DOI: 10.1103/PhysRevB.70.174443 PACS number(s): 75.50.Cc, 75.30.Kz, 76.60.Jx

## I. INTRODUCTION

Intrinsic phase separation in doped transition metal oxides is found to be important in determining unusual properties in these materials. An important example is colossal magnetoresistance in the manganites. Phenomena of this kind have attracted considerable experimental and theoretical interest. The high-$T_C$ cuprates and the cobaltites provide further examples of microscopic phase separation effects. Recent theoretical work[1,2] has provided insight into the mechanisms that give rise to nanoscale phase separation in these systems.

Experimental evidence[3,4] obtained for Sr-doped cobaltites, $La_{1-x}Sr_xCoO_3$, has confirmed that ferromagnetic (FM) and nonferromagnetic (NFM) phases coexist for a wide range of dopant levels. Co ions are present in different charge and spin states leading to a rich variety of properties as a function of temperature and applied magnetic field, including large negative magnetoresistance for $x<0.2$ (Refs. 5 and 6) and a very large anomalous Hall effect.[7] Phase diagrams for the doped system have been proposed by a number of workers,[8–11] and show a metal-insulator (MI) transition at $x=0.18$ and a Curie temperature $T_C$ close to 240 K for $x>0.3$. In the metallic region, FM coupling is attributed to double exchange between $Co^{3+}$ and $Co^{4+}$ ions, similar to the double exchange mechanism in the doped manganites. Neutron and transport measurements[12] suggest that magnetic polarons are formed in Sr-doped samples as $T$ is raised and passes through $T_C$.

The crystal structure of $LaCoO_3$ is almost cubic, with a small rhombohedral distortion, and has the space group $R3c$. For $La_{1-x}Sr_xCoO_3$ the rhombic distortion decreases with increasing $x$, eventually vanishing for $x=0.5$. In undoped $LaCoO_3$ competing crystal field splitting and Hund's rule coupling effects lead to a small gap between $t_{2g}^6e_g^0(S=0)$, low-spin (LS), and $t_{2g}^5e_g^1(S=1)$, intermediate-spin (IS), states. Magnetic susceptibility measurements[13] and photoemission spectroscopy[14] show a transition of Co ions from LS to IS states in the temperature range 30–100 K as a result of thermal excitation. At temperatures above 100 K Curie-Weiss susceptibility behavior is observed.

For Sr-doped samples the $Co^{3+}$ IS states are stabilized at all temperatures in the vicinity of dopant atoms.[13] The MI transition at $x=0.18$ corresponds to a percolation threshold involving metallic FM clusters. Magnetization and ac susceptibility measurements[11] on selected samples have shown that spin-glass (SG) or cluster-glass (CG) behavior is observed as the temperature is lowered below $T_C$. Field cooled (FC) and zero-field cooled (ZFC) magnetization data[11,15] show marked differences at temperatures well below $T_C$ that may be explained in terms of SG or CG properties. The FC $M(T)$ curves can be fitted using a Brillouin function with $S=1$.[11] This is consistent with the $Co^{3+}$ ions being in the IS state and $Co^{4+}$ ions in either the LS or IS states.[3,11,10,16] Neutron diffraction has shown that temperature-dependent local lattice distortions, specifically involving Co-O bond angles and lengths, are present in doped material.[3] Elastic and inelastic neutron scattering experiments[16] provide evidence for both static and dynamic Jahn-Teller (JT) distortions depending on the dopant concentration. Long-range elastic interactions between JT sites may be important in determining the SG properties.[16]

While phase separation has been established for high quality doped cobaltite samples, many questions relating to the underlying mechanism remain to be answered. Direct evidence for hole-rich and hole-poor regions, based on high-resolution transmission electron microscopy images, has been obtained in samples with $x=0.15$ and $x=0.30$.[3] The evolution with temperature of the distinct FM and NFM phases has not previously been studied in detail at the microscopic level.

$^{59}Co$ NMR spin echo experiments have provided information on the coexistence of FM and NFM phases for tempera-

 

tures in the range 2–25 K for both metallic and insulating samples.[4] Measurements at higher temperatures were not carried out since the $^{59}$Co spin-spin relaxation time $T_2$ decreases with $T$ and above 25 K becomes so short that spin echo detection is no longer possible. The ZF and high-field (HF) $^{59}$Co results, taken together, have shown that phase separation, as determined using the areas of NMR spectra, is not sensitive to the field used or to the cooling protocol (FC or ZFC) followed. $^{139}$La NMR offers an alternative approach to the study of phase separation in this system. Previous ZF $^{139}$La NMR experiments in doped material[17] have shown that the transferred hyperfine coupling at the La sites corresponds to a resonance frequency of ~15 MHz in the FM regions. Few previous high-field $^{139}$La measurements appear to have been carried out on doped or undoped material. The present work has used high-field $^{139}$La NMR to investigate phase separation effects in $La_{1-x}Sr_xCo_3$ for a number of dopant concentrations $x$ in the range 0.1 to 0.3, at temperatures up to 300 K. For comparison purposes some measurements have been made on an undoped sample and a lightly doped sample.

## II. EXPERIMENTAL PROCEDURES

The samples were prepared by solid-state reaction. Details of material preparation and characterization have been given previously.[4,11] The samples consisted of polycrystalline material with an average grain size of 10 μm. Samples with $x$ values 0, 0.03, 0.1, 0.18, and 0.30 were used in the investigation.

The $^{139}\mathrm{La}\left(I=\frac{7}{2}\right)$ NMR spin echo experiments were carried out using a pulsed spectrometer with a tuned variable temperature probe. At a chosen temperature, spectra were obtained from the spin echo envelope, at a fixed frequency of 87.5 MHz, by sweeping the magnetic field over the range 10–15 T using a superconducting magnet. Signal averaging enhanced the signal-to-noise ratio. Experiments at higher fields, up to 22 T, were carried out using a resistive Bitter magnet. Temperatures were controlled and measured using a Lakeshore controller with calibrated sensor. No enhancement of the nuclear signal due to FM effects was found.

The signal amplitude was monitored for a range of rf power settings and pulse lengths to ensure that optimal spin echo conditions were achieved. Spin-spin and spin-lattice relaxation rates were measured as a function of field and temperature. In analyzing the recovery of the nuclear magnetization due to spin-lattice relaxation processes, use was made of either single exponential or multiexponential $I=7/2$ master equation fitting procedures. Further details are given with the results.

## III. RESULTS AND DISCUSSION

### A. Undoped and lightly doped material

Figures 1(a) and 1(b) show $^{139}$La field scan 87.5 MHz spectra taken at 20 K for $LaCoO_3$ and $La_{0.97}Sr_{0.03}CoO_3$ samples, respectively. A classic quadrupolar split powder spectrum is obtained for the undoped material. The quadrupolar coupling frequency, obtained by fitting the $I=7/2$ spectrum, using standard second-order expressions and assuming axial symmetry,[18] is $\nu_Q=1.7$ MHz, in agreement with the value obtained by Itoh and Natori.[19] A spectrum obtained at 120 K showed the same structure as the 20 K spectrum with a small Knight shift. The $^{139}$La Knight shift as a function of temperature has a form similar to that of the magnetic susceptibility, rising from zero for $T$ below 20 K to a maximum of 0.56% at 115 K.[19] The form of the susceptibility curve as a function of temperature has been discussed by Yamaguchi *et al.*[13] using a mean-field approach. Recent electronic structure calculations[20] have provided a description of the temperature induced LS-IS transition and the associated changes in the magnetic properties revealed by experiment.

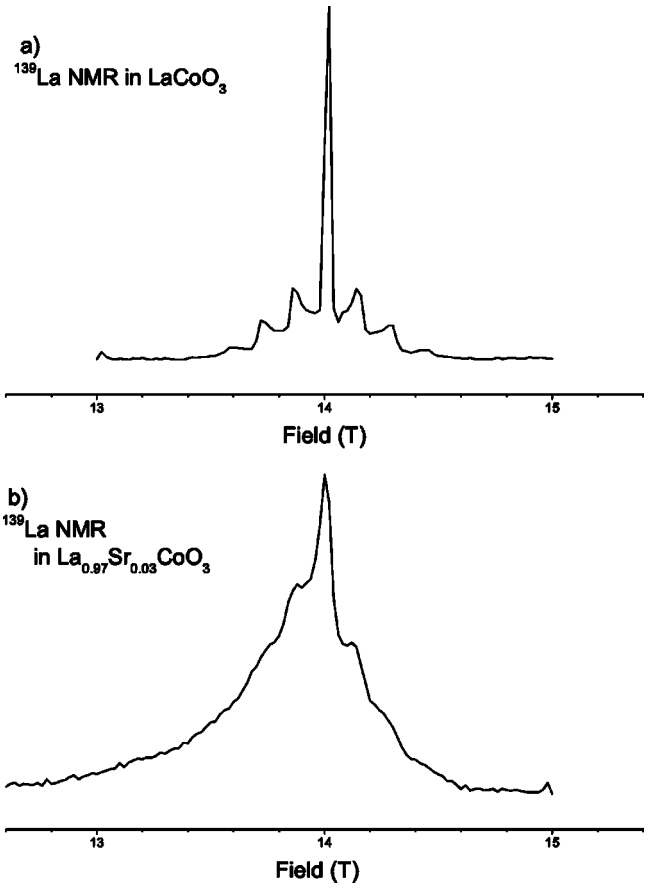


FIG. 1. (a) $^{139}$La spectrum for $LaCoO_3$ at 20 K. (b) $^{139}$La spectrum for $La_{0.97}Sr_{0.03}CoO_3$ at 20 K.

The 20 K spectrum for the lightly doped material, with $x=0.03$, shows significant broadening compared to the $x=0$ spectrum. This is in part attributed to a distribution of quadrupolar coupling frequencies due to local lattice distortions produced by Sr doping. Changes in the quadrupolar interaction should produce a symmetrically broadened line shape. A low-field tail on the spectrum is observed which may be attributed to a local field distribution. Magnetic susceptibility measurements[13] together with infrared spectroscopy[21] have revealed a marked change in the low temperature $\chi$ behavior between undoped and very lightly Sr-doped samples ($x=0.002-0.01$). In the latter, the highly enhanced $\chi$ for $T<100$ K is attributed to localized magnetic polarons with high spin numbers.[13]

Thus, small amounts of hole doping lead to a local collapse of the LS-IS gap in regions surrounding dopant ions, with the Co ions in the IS state.[13] The observed NMR line shape for $x=0.03$ is consistent with the $^{139}$La nuclei experiencing a distribution of local fields due to variations in the local $\chi$ values produced by the random location of Sr ions. Superparamagnetic clusters have been suggested as precursors to the FM clusters found at higher Sr concentrations.[3] At temperatures close to and above the Curie temperature, it has been suggested that magnetic polarons become important as the FM regions tend to disorder.[3,12] The present work provides further evidence for magnetic correlation effects being significant for a range of dopant concentrations and temperatures. This feature is discussed below in the context of the highly doped samples.

Spin-lattice relaxation measurements have been made as a function of temperature for the undoped, $x=0$, sample. Figure 2 shows the transition rate $^{139}$W versus $1/T$. The values for $^{139}$W were obtained by fitting the observed nuclear magnetization recovery curves using the master equation for magnetic relaxation of the central $(|\mp\frac{1}{2}\rangle \leftrightarrow |\pm\frac{1}{2}\rangle)$ transition in an $I=\frac{7}{2}$ system. A dramatic increase in the relaxation rate occurs above 30 K, with a maximum around 70 K and the rate decreasing at higher temperatures. This temperature range coincides with that in which Co ions undergo $S=0$ to $S=1$ spin-state transitions.[13,14,20] Magnetic susceptibility ($\chi$) data,[13] with a constant scale factor, are shown for comparison purposes in Fig. 2. The relationship between $^{139}$W and $\chi$ is discussed below.

$^{139}$La nuclei experience a fluctuating transferred hyperfine interaction, induced by the spin-state transition in neighboring Co ions, which gives rise to nuclear relaxation. The Hamiltonian for the $^{139}$La system is

$$H = H_Z + H_Q + H_{HF}, \tag{1}$$

with $H_Z$ and $H_Q$ the Zeeman and quadrupolar Hamiltonians, respectively, and $H_{HF}$ the transferred hyperfine interaction due to spins on adjacent ions. In the slightly distorted cubic structure each La ion occupies a *body-center* site. $H_{HF}$ may be written in terms of $B$, the hyperfine coupling between a nuclear spin $\boldsymbol{I}$ and neighboring electron spins $\boldsymbol{S}_i$ on sites $i$, as

$$H_{HF} = B\,\Sigma_i \boldsymbol{I}\cdot\boldsymbol{S}_i. \tag{2}$$

$H_{HF}$ is assumed isotropic and fluctuates, with short correlation time $\tau$, between zero for $S=0$ and a maximum value for $S=1$, giving rise to a small temperature-dependent paramagnetic Knight shift in the nuclear resonance spectrum and inducing nuclear relaxation transitions. We ignore relaxation contributions due to quadrupolar mechanisms since these will be small at the temperatures of interest here.

If it is assumed that correlations among the $S$ spins may be ignored and that the correlation function of the resultant fluctuating hyperfine field due to spin-state transitions decays exponentially with time, the nuclear relaxation transition rate may be written as[18]

$$^{139}\mathrm{W} = [2\ zP_i(T)B^2/3\hbar^2]S(S+1)[\tau/(1+(\omega_I-\omega_S)^2\tau^2]. \tag{3}$$

$P_i(T)$ is the probability of finding an $S$ spin in site $i$, with $z=8$ the number of neighboring sites, while $\omega_I-\omega_S$ is the difference between the nuclear and electron Larmor frequencies. Since $\omega_I \ll \omega_S$, we drop $\omega_I$ in the denominator. $\tau$ is the correlation time of spins in the $S=1$ state.

It is necessary to consider whether the maximum observed at 70 K in the measured transition rate plot, shown in Fig. 2, is linked to the maximum in the spectral function in Eq. (3). Detailed calculations show that this is not the case. The energy of a Co ion in the $S=1$ (IS) state in an applied magnetic field $H$, allowing for exchange coupling $J$ with nearest neighbors in the IS state, is

$$E = g\mu_B Hm - 2zJ\langle S\rangle m + \Delta, \tag{4}$$

with the electron $g\approx 2, m=0,\pm 1$ and $\mu_B$ the Bohr magneton. Yamaguchi *et al.*[13,21] have assumed an antiferromagnetic interaction between neighboring spins in their mean-field treatment of magnetic susceptibility results, but Zobel *et al.*[22] have found that they can fit their susceptibility data using an approximation in which $J$ is assumed negligible. In order to simplify the present discussion, we neglect any exchange interactions in comparison to the gap energy $\Delta\sim 180$ K.

The probability factor in Eq. (3) is given by

$$P_i(T) = \nu\Sigma_m \exp[(g\mu_B Hm-\Delta)/k_BT]/Z, \tag{5}$$

with orbital degeneracy $\nu$, spin gap $\Delta$, and partition function $Z$. In the high-temperature approximation this becomes, measuring $\Delta$ in K,

$$P_i(T) = \nu(2S+1)e^{-\Delta/T}/Z, \tag{6}$$

with $Z=1+\nu(2S+1)e^{-\Delta/T}$.

The recent magnetic susceptibility measurements[22] have shown that orbital nondegeneracy applies in the IS state for $T<500$ K, and we have therefore chosen $\nu=1$. For $\Delta=180$ K,[22] Eq. (6) predicts that $P_i(T)$ increases rapidly with $T$ between 30 and 100 K before tending towards a limiting high $T$ ($T<300$ K) value of 0.66. Figure 2 permits a comparison to be made of the relaxation rate $1/T$ dependence with that of the magnetic susceptibility.[13] The similarity in form below 70 K is striking and points to an underlying connection. Yamaguchi *et al.*[21] and Zobel *et al.*[22] have analyzed their $\chi$ data using a model that incorporates LS to IS spin-state transitions with energy gap $\Delta$ between the $t_{2g}{}^6e_g{}^0(S=0)$ ground state and the $t_{2g}{}^5e_g{}^1(S=1)$ state.

The susceptibility may be written as[22]

$$\chi(T) = [Ng^2\mu_B{}^2/3k_BT][\nu S(S+1)(2S+1)e^{-\Delta/T}/Z]. \tag{7}$$

If in Eq. (3) we assume $\omega_S\tau \ll 1$ and make use of Eq. (5), we obtain

$$^{139}\mathrm{W} = [32/3(B/\hbar)^2]\{\nu S(S+1)(2S+1)e^{-\Delta/T}/Z\}\tau. \tag{8}$$

It is clear that Eqs. (7) and (8) have similar forms, leading to the following relationship

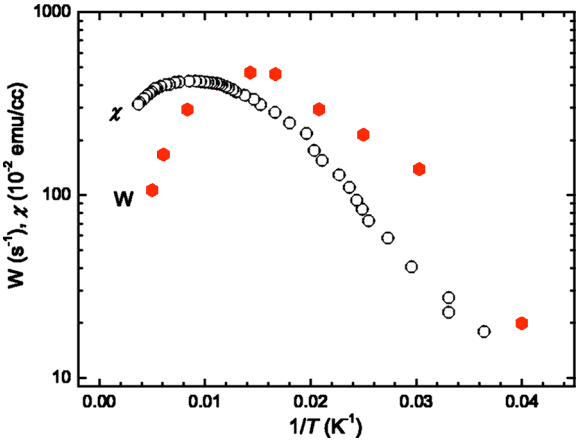


FIG. 2. (Color online) Spin-lattice relaxation rate $^{139}$W versus $1/T$ for $LaCoO_3$ and scaled (100 times smaller) $LaCoO_3$ magnetic susceptibility $\chi$ vs $1/T$ ($\chi$ data are from Ref. 21).

$$^{139}\mathrm{W} = C\ \chi(T)T\ \tau, \tag{9}$$

with $T$-independent factors collected into $C$. The Knight shift may similarly be written as

$$K = Bz\ \chi(T)/Ng\mu_B, \tag{10}$$

which shows that $K$ tracks $\chi(T)$ as observed.[19]

The hyperfine frequency contribution per Co neighbor, $B/\hbar$, may be estimated using the static hyperfine coupling in the ferromagnetic phase in Sr-doped material. (This implicitly assumes that $Co^{3+}$ and $Co^{4+}$ ions involved in double exchange have similar transferred hyperfine couplings at the La sites.) The value obtained using the frequency shift given in Sec. III B is 1.7 MHz per Co ion. The correlation time $\tau$ may be determined using this value in Eq. (6) and taking $\Delta = 180$ K.

Figure 3 shows values of $\tau$ in the range $10^{-12}$ to $10^{-13}$ s, obtained from the relaxation data using Eq. (8), plotted as a function of $1/T$. Below 70 K, $\tau$ decreases roughly linearly with increasing $T$, while at higher temperatures the decrease with $T$ becomes more rapid. The linear dependence is consistent with $\tau \propto 1/T$. Insertion of an inverse $T$ dependence for $\tau$ in Eq. (9) gives a direct proportionality between the relaxation rate and the magnetic susceptibility, as implied by the experimental results in Fig. 2 for temperatures below 70 K.

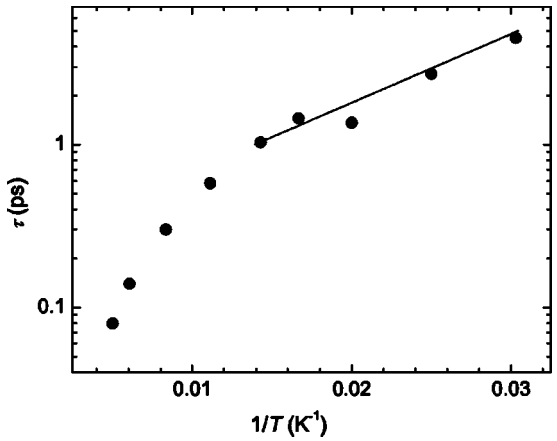


FIG. 3. Correlation time $\tau$ for the $S=1$ thermally excited state in $LaCoO_3$ versus $1/T$. The $\tau$ values have been extracted from the measured $^{139}$La relaxation data assuming a spin gap $\Delta$ of 180 K.

In order to understand the correlation time behavior with temperature, it is necessary to consider the phonon processes that are responsible for spin-state transitions. Ignoring possible $J$ couplings, as discussed above, Eq. (4) shows that two energy gaps are important: $\Delta = 180$ K and $\delta = g\mu_B H = 20$ K ($H = 14$ T) within the Zeeman split $S=1$ multiplet. Correspondingly, using expressions for relaxation due to spin-phonon processes,[23] we have

$$1/\tau = 1/\tau_\Delta + 1/\tau_\delta, \tag{11}$$

with the correlation times for the two independent processes given by

$$1/\tau_\Delta = P\ \Delta^3[1/(1 - e^{-\beta\Delta})]$$

and

$$1/\tau_\delta = P'\ \delta^3[1/(1 - e^{-\beta\delta})].$$

$P$ and $P'$ are the spin-phonon coupling constants for the two processes that are considered with $\beta = 1/k_B T$. The coupling constants may be estimated within a Debye model approach, but such estimates are of dubious value in view of the complex lattice dynamics of the $LaCoO_3$ system. Clearly, $\tau_\delta \leqslant \tau_\Delta$ since $\tau_\Delta$ is the characteristic lifetime of the excited state. In the temperature range 30 to 70 K the system is in the high-temperature limit for $\delta$-transitions within the $S=1$ multiplet but in the low-temperature limit for the $S=0$ to $S=1$ $\Delta$-transitions. Expansion of the Planck distribution in the high-temperature limit leads to a $1/T$ dependence for $\tau_\delta$. Our results suggest that for $T < 70$ K $\tau_\delta < \tau_\Delta$, giving rise to the observed linear behavior in Fig. 3. At higher temperatures, $\tau_\Delta$ presumably becomes sufficiently short that both times are important in Eq. (11), leading to a nonlinear decrease of $\tau$ with $T$.

As discussed above, our analysis ignores possible exchange couplings between the $S=1$ spins. Inclusion of couplings of this kind, within a mean-field approach, is possible but has not been attempted in view of the uncertainties in the magnitude of these couplings. The information on correlation times for the spin-state transitions presented in Fig. 3 is not expected to be altered in any significant way by exchange effects at the temperatures of interest. The peak in the relaxation rate versus $T$ curve may be understood as not due to a maximum in the spectral function given in Eq. (3), nor the maximum in $\chi(T)$, but is due to competition between the rapid increase in the probability of occupation of the $S=1$ state, in the range 30 to 100 K, and the steady decrease in the correlation time $\tau$ with temperature in analogy with high $T_C$ cuprates.

### B. Highly Sr-doped material

Figure 4 shows representative $^{139}$La field scan spectra (at 87.5 MHz) as a function of $T$, between 2 and 280 K for $x = 0.1$, 0.18, and 0.30: $x = 0.1$ is located in the insulating phase, $x = 0.18$ at the MI phase boundary, and $x = 0.30$ in the

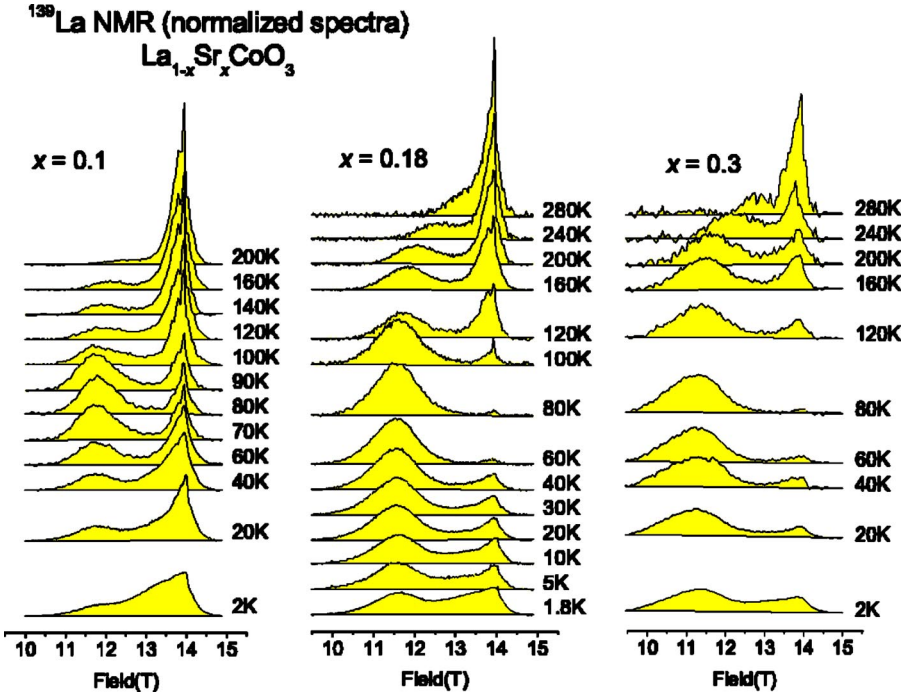


FIG. 4. (Color online) $^{139}$La 87.5 MHz spectra as a function of $T$ for $x=0.1$, 0.18, and 0.30.

ferromagnetic metallic phase.[11] The areas have been normalized to allow for changes in the Boltzmann factor. This procedure was checked for consistency by plotting the areas against $1/T$. Similar spectra were obtained at higher fields for $x=0.10$ and 0.18. Figure 5 shows an example of an 87.5 MHz spectrum for $x=0.10$. All the spectra exhibit multiple peaks in the field ranges shown. In most of the discussion that follows emphasis is placed on the 87.5 MHz, 10-15 T

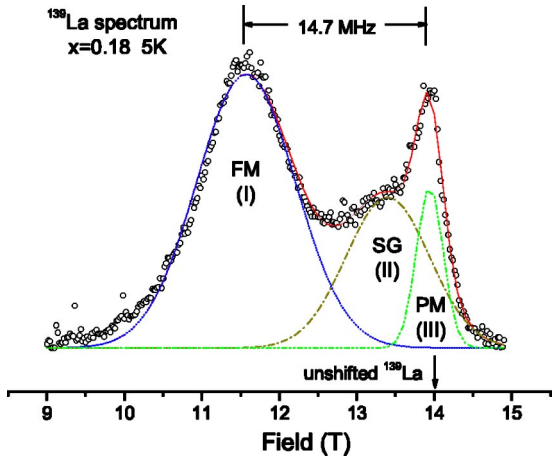


FIG. 5. (Color online) Gaussian fits to $x=0.18$ spectra for $T=5$ K. This fitting procedure was used for all temperatures and concentrations. The relative areas are proportional to the relative concentrations at a given temperature. To compare for different temperatures they must be scaled by the Boltzmann factor. The splitting between the low-field peak (I) and the unshifted peak (III) corresponds to the observed zero external field $^{139}$La NMR frequency, establishing that it comes from the ferromagnetic regions in the sample.

results. The data obtained at higher fields in the 18–22 T range are consistent with the 10–15 T results and no field dependence of the phase separation properties is apparent in our results. While we cannot exclude a possible field dependence of the FM phase fraction at low magnetic fields, the present high-field (10-20 T) measurements, taken together with our previous $^{59}$Co ZFC and FC results,[4] suggest that such effects are likely to be small. The spectra were fit using three Gaussian curves as shown in Fig. 5. For this discussion the peaks are labeled I, II, and III with increasing field. Lorentzians gave slightly better fits above 160 K, and were used in that temperature range to find the relative areas, although the differences were small. The arrow shown in Fig. 5 corresponds to the field, (13.95 T) for the unshifted $^{139}$La spectrum at a frequency of 87.5 MHz using $^{139}\gamma = 6.014$ MHz $T^{-1}$. It can be seen that the center frequency of peak III lies very close to the unshifted value. This suggests that peak III, which is relatively narrow compared to the other two peaks, corresponds at low $T(<30$ K) to paramagnetic LS (PM) phase regions in the sample. Previous $^{59}$Co NMR results[17,24] have provided evidence for the presence of a LS phase with a Knight shift of $\sim 2\%$ in agreement with the low temperature value found in undoped material. This shift is discussed in greater detail below. The short $^{59}$Co spin-spin relaxation time prevented measurements at higher temperatures where LS to IS spin-state conversion of Co ions occurs.

The low-field peak I is broad and is centered at a field of 11.5 T, which is 2.45 T lower than the center of peak III. Using the $^{139}\gamma$ value this field shift corresponds to a frequency shift of 14.7 MHz, close to the transferred hyperfine field value obtained in ZF NMR experiments. We therefore identify peak I with spectra from $^{139}$La in FM regions.

In FM regions, the resonance field for a given nucleus $i$ may be written as

$$\boldsymbol{B} = \boldsymbol{B}_o + \boldsymbol{B}_{hf}^i, \tag{12}$$

where $\boldsymbol{B}_o$ is the applied field and $\boldsymbol{B}_{hf}^i$ the hyperfine field at $i$ given by the product of the hyperfine coupling and the mean electron spin $\langle \boldsymbol{S} \rangle$, which is proportional to the magnetization $M$ in the region containing the nucleus. The large linewidth observed for this peak is attributed to a distribution of hyperfine fields in the FM components. It is interesting to note that the linewidth increases with increasing $x$. The downfield shift of peak I means that the transferred hyperfine field is aligned parallel to the applied field.

The fitted peak II lies at an intermediate field between the PM phase almost unshifted line, and the FM hyperfine shifted line. This spectral component has a shift which is less than half that of the FM peak I but a comparable breadth. We tentatively assign this phase as a SG phase, although the precise nature is not clear and is likely to involve a distribution of local environments. The transferred hyperfine field is clearly smaller in the SG phase than in the FM phase. Previous work suggests that this phase involves interactions between small hole-rich clusters mediated by a LS matrix.[3,8,9]

Some uncertainty in the sum of Gaussians fit of peaks I and II must be considered, because of spectral overlap. However, consistent results are found in all cases when the procedure is used in a systematic way. The numbers of La ions in the different phases are proportional to the areas under the corresponding NMR spectral peaks. For all three concentrations there are common features in the changes in peak center fields and areas, which are observed as $T$ is raised.

By following changes in peak areas with temperature, information on the evolution of the concentration of the separate phases was obtained. The variations in the area under the individual peaks with $T$, for the three concentrations studied, are shown in Fig. 6. Similarities in the phase evolution behavior for the three concentrations are clear, with an initial growth of the FM phase concentration with increasing temperature, followed at higher temperatures by a decrease. Further discussion of these results is given below.

Figure 4 shows that the transferred hyperfine field for peak I decreases with $T$ for all three concentrations as expected. Figure 7 shows the reduced field shift $\Delta H/\Delta H_o$, which is proportional to the reduced magnetization $M/M_o$, versus reduced temperature $t=T/T_C$ for $x=0.18$. $\Delta H_o$ is the extrapolated $T=0$ K shift. The fitted curve shown is the Brillouin function for $S=1$ as used in fitting conventional FC magnetization data.[11] The upper and lower limits of the different reported Curie temperatures $T_C$ for $x=0.18$, 160 (Refs. 8 and 11) –240 (Refs. 9 and 10) K, were taken from published phase diagrams. While the reduced data do not agree with the Brillouin function for $T_C=160$ K, which is the value expected from $M(T)$ and resistance data for $x=0.18$,[11] we find that for $T_C=240$ K (the maximum for $x$ approximately 0.5) the agreement with the Brillouin function is fairly good over a large range of reduced temperatures. The discrepancy in $T_C$ values is not currently understood. Our results suggest that the macroscopic measurements lead to a lower $T_C$ than is found from the microscopic NMR measurements. This points to small FM regions having relatively high $T_C$ values close to the value found in larger FM regions. At the highest

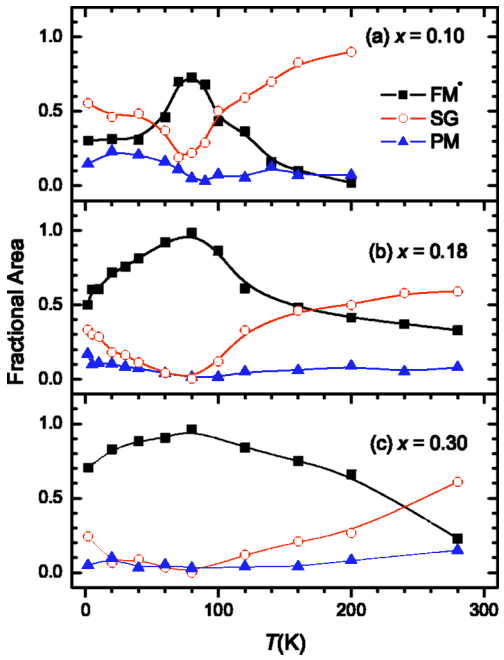


FIG. 6. (Color online) $^{139}$La Gaussian areas (proportional to the relative concentration) for peaks I (FM or possibly spin polarons at high temperature), II (SG), and III (PM) versus $T$ for (a) $x=0.10$, (b) $x=0.18$, and (c) $x=0.30$. The center field for peak I shifts with $T$ and for $T>200$ K is not possible to differentiate between FM shifts and effects due to superparamagnetic clusters or spin polarons.

$t$ values, in the vicinity of $t=1$, the data points show a departure from the fitted Brillouin function with a gradual decrease in the normalized shift persisting above the nominal $T_C$. This feature is discussed below.

The center field for peak III agrees with the unshifted $^{139}$La value, to within an uncertainty of 0.5%, and shows only a weak $T$ dependence, consistent with a small paramagnetic shift (not shown in the figures) at all $x$ values studied.

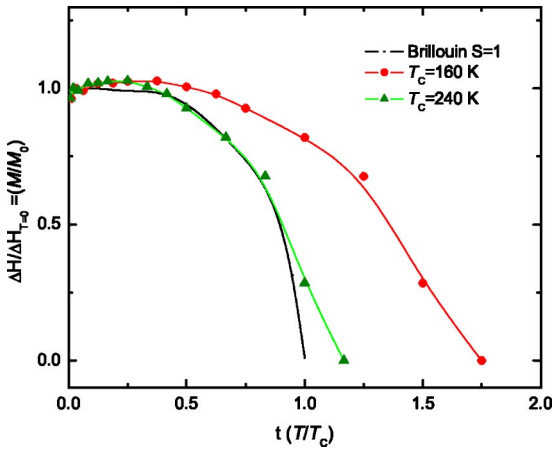


FIG. 7. (Color online) Center field for peak I ($f=84.2$ MHz) versus reduced temperature $T/T_C$ for $x=0.18$. The solid curves are Brillouin functions for $S=1$ with $T_C=160$ and 240 K, respectively. Upper and lower possible values for $T_C$ have been used to scale the experimental temperature values. The curves through the scaled data points are to aid the eye.

The lack of any measurable shift at low $T$ is consistent with these La nuclei being in a Co LS phase. As $T$ is raised, Co (III) ions in the LS paramagnetic PM phase undergo a spin-state transition to an IS state, between 30 and 100 K, corresponding to the energy gap of 180 K between $t_{2g}^6 e_g^0$ (LS) and $t_{2g}^5 e_g^1$ (IS) states. $^{59}$Co NMR experiments on undoped $LaCoO_3$ have shown a temperature-dependent resonance shift with a low-temperature (LS) value of 2.1%, attributed to a Van Vleck orbital contribution, rising to over 5% at the maximum around 100 K.[17] The much smaller shifts for $^{139}$La, found in the present experiments, are consistent with the small shifts due to transferred hyperfine coupling found in the undoped material at temperatures above 40 K.[19] As mentioned in Sec. III A above, the magnetic susceptibility shows a peak at 100 K, reflecting the LS to IS transition, with Curie-Weiss behavior at higher temperatures.[8,13,25]

The behavior with $T$ of the center field for peak II is less clear than for the other two peaks. The amplitude of this peak is strongly $T$ dependent and the behavior is consistent with partial conversion of SG phase to FM phase with increasing temperature, as discussed below.

Figure 6 shows the areas of peaks I, II, and III expressed as a fraction of the total area under the spectrum, as a function of $T$. For all three $x$ values, the fraction of the sample associated with the FM (peak I) phase shows an increase while that due to the SG phase (peak II) shows a decrease as $T$ is raised from 2 to 80 K. Above 80 K this trend is reversed with the FM component steadily decreasing in importance. The growth of the FM phase is consistent with partial conversion of the SG phase to FM over the temperature range in which LS to IS spin-state conversion occurs, as discussed above. The fractional area of peak I, corresponding to the PM phase, remains roughly constant with temperature.

The $^{139}$La relaxation time results in the highly doped material will not be presented in great detail, partly because the spin dynamics of this system have previously been discussed at some length based on $^{59}$Co relaxation time measurements.[26] A brief discussion of the principal findings are given here. The observed $^{139}$La spin-lattice relaxation recovery curves for $x \geqslant 0.1$ were multiexponential at all temperatures studied, for all three phases. The $I=\frac{7}{2}$ master equation did not provide a satisfactory fit to the recovery curves. The multiexponential form of the recovery curves is consistent with a distribution of local environments. For the FM and SG regions the $T_1$ values decreased with temperature, pointing to a mechanism involving fluctuating moments whose correlation times are changing with temperature as discussed previously for $^{59}$Co relaxation in NFM phases.[26] The observations in the PM region are consistent with LS to IS spin state conversion processes becoming important as $T$ is increased. Figure 8 is a plot of the relaxation rates for $x=0$ (undoped) and $x=0.18$ samples. Similar fitting procedures involving a single exponential were used for consistency in the comparison of relaxation rates although, as has been pointed out in Sec. III A, the undoped sample recovery curves were well fitted using the master equation. A clear similarity in the shapes of the relaxation rate curves shown in Fig. 8 is evident, and this proves that the LS to IS transition occurs in the PM phase of the highly doped samples. The maxima in the rates for $x=0$ and $x=0.18$ are at roughly the same temperature. The gradual decrease in the relaxation rate at low temperatures is attributed to a mechanism involving paramagnetic impurities, or oxygen vacancies. Recent work has shown that oxygen nonstoichiometry effects in $LaCoO_3$ can give rise to the existence of interacting magnetic excitons, which could play a role here.[27]

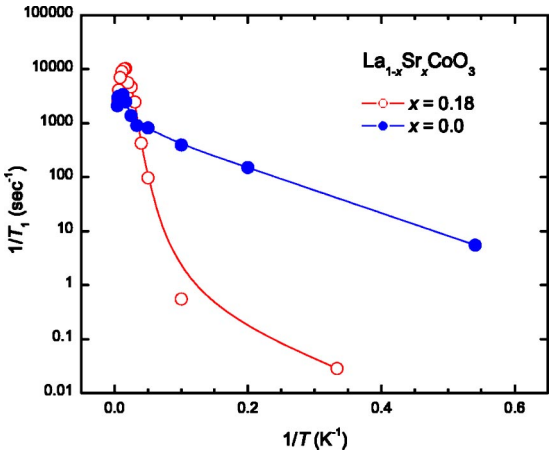


FIG. 8. (Color online) $^{139}$La spin-lattice relaxation rates for $LaCoO_3$ and $La_{1-x}Sr_xCoO_3(x=0.18)$ versus $1/T$.

The present findings concerning phase separation and phase conversion with temperature raise important questions concerning the phase diagrams that have previously been presented for the Sr-doped cobaltites. It is clear from our work, and from previous investigations,[3,4] that the mixed phase nature is intrinsic to this material over a wide range of dopant concentrations. Evidence for phase separation in $Nd_{1-x}Sr_xCoO_3$ has also recently been obtained using NMR.[28] While it may be useful to represent the average macroscopic properties as a function of $x$ and $T$ it is necessary to appreciate that these oxide systems, at any nominal $x$, may have a distribution of properties resulting from the nano-scale distribution of phases.[3,26]

It is convenient in attempting explanations for the present results to consider the low temperature ($T \leqslant 80$ K) and high temperature ($T > 80$ K) regimes separately.

### *1. $T \leqslant 80$ K*

A qualitative explanation for the initial growth of FM regions, for a given $x$, with increasing $T$ followed by a decrease at higher $T$ may be given as follows. We suggest that spin state conversion in NFM regions adjacent to FM regions leads to the growth of the FM regions through local transformation to the more ordered state. Local static or dynamic JT-type distortions, involving Co-O bond parameters, are likely to play a role in the FM phase growth process as suggested previously.[3,12] For sufficiently large $x$ (0.1–0.3 in the present experiments) interconnection of isolated FM regions, which at low $T$ are separated by SG material, may occur. The proposed conversion mechanism is consistent with disorder effects, associated with local variations in hole concentrations, playing a role in the process. Both Co ion spin-state conversion and local JT distortions that occur with increasing temperature in adjacent SG regions may drive the

SG to FM conversion. This proposed growth process involves an increase in the spin correlation length in the FM regions.

Pulsed neutron diffraction data[10] have provided evidence for two types of Co-O bonds in the range 15–300 K. Co (III)(LS)-O bonds are shorter than $Co^{3+}$(IS)-O bonds. The pulsed neutron experiments in addition show that interaction of lattice and charge dynamics can lead to local dynamic distortions. The present NMR results show that thermal effects can convert SG regions into FM regions.

As the temperature is lowered below 100 K, our results show that FM regions tend to break up into FM plus SG regions possibly linked to IS to LS freeze-out. For the case of magnetoelectronic phase separation due to direct inhomogeneities in hole doping, these effects are likely to occur in regions with hole concentrations intermediate between so-called Sr-rich and Sr-poor. The FM-SG phase transformation behavior with temperature is reversible, as shown by warming and cooling experiments.

The theoretical density functional calculations,[20] which allow for spin polarization, suggest that hole doping stabilizes the IS state. While it is difficult to suggest a model for the SG to FM conversion, as observed in the present experiments at temperatures in the range 40 to 100 K, it is likely that a delicate interplay of spin and local structural mechanisms is important in the conversion process.

#### 2. $T > 80$ K

At higher temperatures, where the FM fraction starts to decrease, the important role of JT distortions[21,29] may be gradually reduced by thermal effects and the FM regions are converted into magnetic polarons in hole-rich regions as suggested by previous work.[3,12] The present results (see Figs. 6 and 7) suggest that clusters of this sort persist at temperatures above $T_C$. This conclusion is drawn on the basis of the low-field shoulder for the spectra shown in Figs. 4 and 6, which persists well above the "bulk $T_C$." If the material were to become a simple paramagnet above $T_C$ a much narrower line would be observed centered on a slightly shifted resonance field value.

As mentioned above, neutron diffraction data[10] has provided evidence for two types of Co-O bonds over a wide temperature range. In a detailed study of $La_{1-x}Sr_xCoO_3$ ($0.1 < x < 0.3$) using neutron diffraction and SANS,[3] the results have shown that for $x = 0.3$ there is a transition from itinerant to polaronic conduction as $T_C$ is approached from below. The Co-O bond length shows an abrupt increase with temperature above $T_C$. The increase in the cell volume leads to a critical concentration of $x = 0.3$ for the transition from itinerant metallic to localized semiconducting behavior for $T > T_C$. Magnetic susceptibility measurements on samples with $x = 0.3$ show a departure from Curie-Weiss behavior at temperatures in the range 240 to 300 K; i.e., just above $T_C$.[12] This finding, together with the neutron data, is interpreted as evidence for segregation into hole-rich regions containing magnetic polarons (or other magnetic entities) and hole-poor paramagnetic regions above $T_C$. The present NMR results provide support for this interpretation. The observed hyperfine shifts giving rise to the low-field peak in the high temperature spectra shown in Fig. 4 are attributed to spin polarons that persist above the transition. These clusters do not appear to contribute significantly to the low-field (<0.1 T) magnetization data for $T > 240$ K,[11] but their effects are evident in the magnetic susceptibility results which show departures from Curie-Weiss behavior below 300 K.[12] It is important to note that the present experiments necessarily involve high magnetic fields that could play a role in determining certain features of the observed magnetic behavior at high temperatures.

At temperatures well below $T_C$ the spectra are dominated by contributions from FM regions. For these FM regions the magnetization follows the expected decrease with $T$ at temperatures as high as 200 K. As the breakup of the FM regions into smaller clusters starts to occur at higher $T$, significant departures from the Brillouin function prediction occur. The behavior in this temperature range is again found to be reversible with temperature.

## IV. CONCLUSION

Measurements of the $^{139}$La NMR spectrum as a function of temperature have provided direct evidence of phase separation in $La_{1-x}Sr_xCoO_3$ for $x = 0.1$, 0.18 and 0.30. The different phases experience different hyperfine fields corresponding to the different local magnetic environments in which they are situated. The results show that all three phases coexist at low temperatures for $x \geqslant 0.1$. The phases are identified as FM, SG, and PM, in agreement with conclusions reached on the basis of previous low-temperature $^{59}$Co NMR results. The proportions of the phases are proportional to the areas under the spectral components. Some interconversion of phases is observed, specifically SG to FM, as the temperature is raised above 30 K.

Measurements on undoped and lightly doped ($x = 0.03$) samples have provided information on the Co ion LS to IS conversion process, which becomes important at temperatures in the range 30 to 100 K. The temperature dependence of the correlation time for the $S = 1$ thermally excited spin state has been determined as $\tau \propto 1/T$ for $T < 70$ K. At higher $T$ the correlation time decreases more rapidly, corresponding to $\tau \propto 1/T^{\alpha}$ with $\alpha > 1$. Spin phonon processes determine the behavior of $\tau$ with $T$. The spectra obtained for the undoped and lightly doped samples show evidence of quadrupolar broadening and paramagnetic shifts. This information is useful in interpreting the spectra obtained for the more heavily doped material.

For $x \geqslant 0$, the FM phase shows a large temperature-dependent hyperfine shift, proportional to the local magnetization, that can be fitted, in reduced form, using a Brillouin function at temperatures up to 200 K. At higher temperatures the FM phase shows a more gradual decrease of hyperfine field than that given by the Brillouin function. While the amplitude of the signal decreases at the higher temperatures, this component persists above the Curie point of around 240 K. This is consistent with FM regions breaking up into spin polarons as the temperature traverses the Curie temperature.

The nature of the phase identified as SG is less clear than for the other two phases. The measured mean shift of

roughly 10% is smaller than that of ~25% for the FM phase but is consistent with the presence of some form of weak magnetic ordering. The large linewidth points to a distribution of local fields. It is likely that this phase corresponds to a spin-glass or cluster-glass component in which frustrated interactions between spins or spin clusters are important. This component shows a marked temperature dependence with gradual conversion into the FM phase occurring as the temperature is raised. It is likely that LS to IS spin-state conversion and changes in local JT distortions play a role in the gradual conversion of the SG to the FM component as the temperature is raised from 40 to 100 K.

The almost unshifted $^{139}$La spectral line observed at the high-field end of the spectrum, and designated PM, is attributed to regions with local atomic environments similar to $LaCoO_3$. At low temperatures the Co ions in these regions are in their LS states. The width of this line is much less than for the other two components, and the Curie law corrected amplitude shows little variation with temperature, as seen from Fig. 6. The behavior is consistent with the $^{139}$La being situated in regions which are either diamagnetic or paramagnetic. The observed shortening of the spin-lattice relaxation time is consistent with fluctuating local fields produced by paramagnetic $Co^{3+}$ ions at temperatures above 30 K which is the temperature at which LS to IS conversion starts to be important in the undoped or lightly doped material.

The present results have revealed details of intrinsic phase separation for three $x$ values in $La_{1-x}Sr_xCoO_3$ and have permitted the evolution of the various phases with temperature to be monitored over the range 2 to 300 K. These findings have important implications for the phase diagrams that have been proposed for the system by other workers. The phase diagrams attempt to capture the average behavior of transport and magnetic properties with $x$ and $T$. It is clear, however, that for any given $x$ there is a distribution of properties corresponding to the distribution of phases that coexist and, furthermore, allowance must be made for interconversion of the two magnetic phases with temperature. These features need to be borne in mind in any discussion of the properties of the material.

## ACKNOWLEDGMENTS

Partial support by the National Science Foundation under cooperative agreement DMR-0084173 and the State of Florida is gratefully acknowledged.

[1] A. R. Bishop, T. Lookman, A. Saxena, and S. R. Shenoy, Europhys. Lett. **63**, 289 (2003).
[2] E. Dagotto, T. Hotta, and A. Moreo. Phys. Rep. **344**, 1 (2001).
[3] R. Caciuffo, D. Rinaldi, G. Barucca, J. Mira, J. Rivas, M. A. Señarís-Rodríguez, P. C. Radaelli, D. Fiorani, and J. B. Goodenough, Phys. Rev. B **59**, 1068 (1999); J. Mira, J. Rivas, G. Baio, G. Barucca, R. Caciuffo, D. Rinaldi, D. Fiorani, and M. A. Señarís-Rodríguez, J. Appl. Phys. **89**, 5606 (2001).
[4] P. L. Kuhns, M. J. R. Hoch, W. G. Moulton, A. P. Reyes, J. Wu, and C. Leighton, Phys. Rev. Lett. **91**, 127202 (2003).
[5] S. Yamaguchi, H. Taniguchi, H. Takagi, T. Arima, and Y. Tokura, J. Phys. Soc. Jpn. **64**, 1885 (1995).
[6] V. Golovanov, L. Mihaly, and A. R. Moodenbaugh, Phys. Rev. B **53**, 8207 (1996).
[7] S. A. Baily, M. B. Salamon, Y. Kobayashi, and K. Asai, Appl. Phys. Lett. **80**, 3138 (2002).
[8] M. Itoh, I. Natori, S. Kubota, and K. Motoya, J. Phys. Soc. Jpn. **63**, 1486 (1994).
[9] M. A. Señarís-Rodríguez and J. B. Goodenough, J. Solid State Chem. **118**, 323 (1995).
[10] D. Louca, J. L. Sarrao, J. D. Thompson, H. Röder, and G. H. Kwei, Phys. Rev. B **60**, 10 378 (1999).
[11] J. Wu and C. Leighton, Phys. Rev. B **67**, 174408 (2003).
[12] R. Caciuffo, J. Mira, J. Rivas, M. A. Señarís-Rodríguez, P. G. Raedelli, F. Carsughi, D. Fiorani, and J. B. Goodenough, Europhys. Lett. **45**, 399 (1999).
[13] S. Yamaguchi, Y. Okimoto, H. Taniguchi, and Y. Tokura, Phys. Rev. B **53**, R2926 (1996).
[14] T. Saitoh, T. Mizokawa, A. Fujimori, M. Abbate, Y. Takeda, and M. Takano, Phys. Rev. B **55**, 4257 (1997).
[15] D. N. H. Nam, K. Jonason, P. Nordblad, N. V. Khiem, and N. X. Phuc, Phys. Rev. B **59**, 4189 (1999).
[16] D. Louca and J. L. Sarrao, Phys. Rev. Lett. **91**, 155501 (2003).
[17] M. Itoh and I. Natori, J. Phys. Soc. Jpn. **64**, 970 (1995).
[18] A. Abragam, *The Principles of Nuclear Magnetism* (Oxford University Press, Oxford, 1961).
[19] M. Itoh and I. Natori, J. Magn. Magn. Mater. **140-144**, 2145 (1995).
[20] P. Ravindran, H. Fjellvag, A. Kjekshus, P. Blaha, K. Schwarz, and J. Luitz, J. Appl. Phys. **91**, 291 (2002).
[21] S. Yamaguchi, Y. Okimoto, and Y. Tokura, Phys. Rev. B **55**, R8666 (1997).
[22] C. Zobel, M. Kriener, D. Bruns, M. Grüninger, T. Lorenz, P. Reutler, and A. Revcolevschi, Phys. Rev. B **66**, 020402(R) (2002).
[23] A. Abragam and B. Bleaney, *Electron Paramagnetic Resonance of Transition Ions* (Clarendon, Oxford, 1970).
[24] Y. Kobayashi, N. Fujiwara, S. Murata, K. Asai, and H. Yasuoka, Phys. Rev. B **62**, 410 (2000).
[25] M. A. Señarís-Rodríguez and J. B. Goodenough, J. Solid State Chem. **116**, 224 (1995).
[26] M. J. R. Hoch, P. L. Kuhns, W. G. Moulton, A. P. Reyes, J. Wu, and C. Leighton, Phys. Rev. B **69**, 014425 (2004).
[27] S. R. Giblin, I. Terry, S. Clarke, T. Prokscha, A. T. Boothroyd, J. Wu, and C. Leighton (unpublished).
[28] A. Ghoshray, B. Bandyopadhyay, K. Ghoshray, V. Morchshakov, K. Bärner, I. O. Troyanchuk, H. Nakamura, T. Kohara, G. Y. Lui, and G. H. Rao, Phys. Rev. B **69**, 064424 (2004).
[29] Y. Tokura, Y. Okimoto, S. Yamaguchi, H. Taniguchi, T. Kimura, and H. Takagi, Phys. Rev. B **58**, R1699 (1998).